Living and nonliving particulate iron in the subtropical North Pacific Ocean

Eleanor S. Bates[1], Nicholas J. Hawco[1]

[1]Department of Oceanography, University of Hawai'i at Mānoa, Honolulu, HI, 96822, USA

Correspondence to: Eleanor S. Bates (esbates@hawaii.edu) and Nicholas J. Hawco (hawco@hawaii.edu)

Abstract. Biogenic and authigenic particulate iron (pFe) are key components of the marine iron cycle, influencing the fate of Fe in the upper ocean. However, their relative contributions to the total pFe pool are challenging to quantify. The chemical leach commonly used to operationally define 'labile' pFe is thought to extract both the biogenic and authigenic phases. To independently determine Fe in biomass, we conducted Fe uptake experiments in the surface mixed layer on 12 cruises in the subtropical North Pacific Ocean. Bulk Fe uptake rates varied ~2.5-fold throughout the year, increasing with increasing *Prochlorococcus* and picoeukaryotes abundances. We used particulate carbon and phosphorus as biomass estimates in combination with Fe:C uptake ratios, finding that both led to overestimations of the biogenic pFe pool (>200% of labile pFe in the surface mixed layer). Using the nucleotide adenosine-5'-triphosphate (ATP) as an alternate estimate of living biomass instead suggested that biotic pFe comprised ~60% of labile pFe in the mixed layer. The remainder of the labile pFe pool, defined as 'authigenic + detrital', dominated the labile pFe pool below the euphotic zone, capturing contributions from detrital organic matter, authigenic minerals, and dust. A comparison of Fe phases between Station ALOHA and the subtropical North Atlantic revealed similar concentrations of dissolved Fe and biotic pFe, but higher authigenic pFe concentrations in the North Atlantic, likely reflecting greater dust deposition. The greater role of biotic pFe in the North Pacific may enable high efficiency Fe recycling, which rivals that observed in Fe-limited ecosystems.

Deleted: Biogenic

Deleted: labile

Deleted: biogenic p

Deleted: biogenic

Deleted: nonliving'

Deleted: biogenic

Deleted: nonliving labile

Deleted: biogenic

1 Introduction

The micronutrient iron (Fe) limits phytoplankton growth in ~30% of the global surface ocean, regulating microbial carbon uptake in these regions (Moore et al., 2013; Moore et al., 2001). Therefore, improving our understanding and modeling of marine Fe cycling is crucial for accurately representing drivers of marine carbon cycling and projecting impacts of future environmental change. Global marine Fe models have historically struggled to reproduce observations of dissolved iron (dFe) (Tagliabue et al., 2016), in part due to uncertainties in the internal cycling of Fe in the surface ocean (Boyd et al., 2017; Tagliabue et al., 2019). Particulate Fe (pFe) phases act as sinks and sources of dFe, exerting a major influence on dFe distributions (Bressac et al., 2019; Hurst et al., 2010; Ohnemus et al., 2019). Chemically labile pFe undergoes both biotic and

abiotic transformations, leading to longer retention in the upper ocean than recalcitrant Fe phases (Bates et al., 2025). However, quantifying the biotic and abiotic components of the labile pFe pool remains a challenge.

Biotic iron recycling is driven by the uptake and subsequent remineralization of Fe by microorganisms. Fe is an essential micronutrient for marine organisms, necessary for many microbial functions including photosynthesis, respiration, nitrogen fixation, and more (Raven et al., 1999; Sunda, 1988). Fe quotas, or biomass-normalized cellular Fe content, have been shown to vary for both cultured and natural phytoplankton communities across taxonomic groups, iron availability, and other environmental conditions such as light availability (Twining et al., 2021; Twining & Baines, 2013 and references therein). Boyd et al. (2015) proposed that biotic pFe pools are often set by the balance of these Fe quotas with rates of Fe recycling, after observing similar biotic pFe concentrations across ecosystems with dFe differing by an order of magnitude. Biotic pFe pools can be challenging to estimate, due to variability in determined Fe quotas based on the methods used (King et al., 2012) and difficulties in quantifying C in living biomass. For the latter, previous studies have used measurements of particulate P (e.g., Sofen et al., 2023) or estimates deriving from biovolume (e.g., Boyd et al., 2015). Alternatively, adenosine-5'-triphosphate (ATP) has been employed as a proxy for living biomass, with studies at Station ALOHA finding just 26-42% of upper ocean particulate carbon is living (Henderikx-Freitas et al., 2021; Karl et al., 2022). Concurrent measurement of Fe quotas and ATP thus could provide reasonable estimates of Fe contained within living cells, or biotic pFe.

Authigenic particulate Fe is thought to form via the aggregation of colloidal size (0.02-0.2 μm) Fe oxyhydroxides, by the adsorption of unchelated Fe onto existing particles, or by the precipitation of Fe oxide coatings from solution (Goldberg, 1954; Gunnars et al., 2002; Honeyman & Santschi, 1989; Landing & Bruland, 1987), all of which arise from the low solubility of Fe(III) in seawater (~0.2 nM; Kuma et al., 1996; Liu & Millero, 2002). When Fe supply is high, the dFe pool often contains a large fraction of colloidal Fe (Bergquist et al., 2007; Wu et al., 2001), which can be scavenged by both lithogenic material (Honeyman & Santschi, 1991; Ye & Völker, 2017) as well as phytoplankton surfaces (Hudson & Morel, 1989; Tang & Morel, 2006; Tovar-Sanchez et al., 2003). The quantification of the authigenic fraction in particulate samples has been difficult as there are currently no methods for direct measurement of the entire authigenic Fe pool. Previous studies have suggested large contributions of authigenic pFe to the labile pFe pool without direct measurement (Black et al., 2020; Marsay et al., 2017; Ohnemus et al., 2019). Recently, estimations of the biogenic pFe fraction have been used in combination with a short acetic acid and hydroxylamine leach accessing the labile pFe pool (Berger et al., 2008), allowing for the calculation of the authigenic pFe fraction by difference (Sofen et al., 2023). Sofen et al. (2023) found that the biogenic pFe pool was often much smaller than the labile pFe pool, and therefore that authigenic pFe was a significant contributor to labile pFe in several ocean basins under both high and low Fe concentrations. The addition of colloidal production of authigenic pFe as a sink of dFe from the surface ocean also improved the ability of a global-scale biogeochemical model to reproduce both temporal Fe observations in the North Atlantic gyre and global dFe observations (Tagliabue et al., 2023), highlighting the importance of this phase in driving upper ocean Fe cycling particularly in regions with high Fe inputs.

Deleted: biogenic

Deleted: biogenic

Deleted: Biogenic

Deleted: biogenic

Deleted: the

Here, we utilize bulk Fe uptake rates and concurrent particulate Fe measurements to explore the distributions and behaviors of the biotic and authigenic + detrital labile pFe pools in the North Pacific Subtropical Gyre. Building off of a recently designed low level double spike technique (Hawco et al., 2022), we performed stable Fe isotope uptake experiments in the surface mixed layer on 12 cruises over three years at Station ALOHA, site of the Hawaii Ocean Time-series (HOT) program. We then compare three potential approaches to quantifying biomass pFe concentrations in the upper 300 m based on the bulk Fe uptake rates. In combination with suspended particulate Fe measurements, we estimate the remainder of labile pFe fraction, defined as authigenic + detrital, and assess differences between the two pools over time and with depth.

Deleted: biogenic
Deleted: nonliving
Deleted: biogenic
Deleted: nonliving

2 Methods

2.1 Sample collection and processing

Samples were collected on 12 Hawaii Ocean Time-series (HOT) cruises to Station ALOHA (22.75°N, 158.0°W) aboard the R/V *Kilo Moana* between May 2021 and September 2023. Collection and processing of water column dissolved and particulate Fe profiles have been previously described (Bates et al., 2025; Bates & Hawco, 2025). Briefly, water column particulate samples were filtered at 0.2 µm and first digested using an acetic acid-hydroxylamine hydrochloride leach to dissolve the chemically labile fraction (pFe_{Labile}; Berger et al., 2008). Lithogenic particulate iron (pFe_{Lith}) was operationally defined by an HF/HNO_3 digest performed sequentially following the labile digest (Planquette & Sherrell, 2012). The sum of the lithogenic and labile fractions represents the total particulate Fe (pFe_{Total}; see Bates et al., 2025).

2.2 Iron uptake incubations

Iron uptake incubations were performed following the low-level double spike procedure described in Hawco et al. (2022), with minor modifications. Four "pre-incubations" were prepared by adding 100 µL of a ~1 µM Fe double spike solution (Fe_{DS}) containing ^{57}Fe and ^{58}Fe to 100 mL of 0.2 µm filtered trace metal clean seawater, recently collected from the surface mixed layer. The pre-incubations were then left in the dark at room temperature for approximately 24 hours to allow the Fe spike to equilibrate with natural Fe-binding ligands. Seawater for the incubations was collected after sunset from the mixed layer (sampled at 25 m depth), following trace metal clean procedures. The incubations were set up in a "clean laboratory van" under red light to avoid light shock to the phytoplankton. The 100 mL pre-equilibrated solution was added to a 2 L acid-cleaned polycarbonate bottle pre-rinsed with filtered seawater, which was then filled with unfiltered trace metal clean seawater. The incubations were performed in triplicate. A control incubation was conducted using 0.2 µm filtered seawater to account for abiotic precipitation of pFe or adsorption of dFe onto the filter. The bottles were placed in an on-deck flow-through incubator, shaded to light levels equivalent to a depth of 25 m and left for 24 hours. The incubations were then harvested via vacuum filtration onto acid-cleaned 0.2 µm Supor filters (47 mm), with the filtrate collected in acid-cleaned 1 L bottles. The filtrate was acidified to pH 1.8 using hydrochloric acid (Fisher Scientific OPTIMA grade) and left

for > 2 months. Laboratory purification of samples and measurement via MC-ICPMS followed the methods described in Hawco et al. (2022), with measurements performed using a Thermo Scientific Neptune at the University of Southern California, using the IRMM-014 standard to define the natural abundance ratio of Fe.

The total mean Fe_{DS} recovered from the dissolved and particulate phases was 55 ± 21 pM, which represents ~12% of the mean mixed layer dFe concentration for these cruises (0.43 ± 0.23 nM). Dissolved Fe turnover times (τ_{FeDS}) and uptake rates (ρ_{dFe}) were calculated following the equations in Hawco et al. (2022):

$$\tau_{Fe_{DS}} = \left(\frac{pFe_{DS}+dFe_{DS}}{pFe_{DS}}\right) \times \Delta t \,, \quad (1)$$

based on the concentrations of the Fe double spike in the particulate and dissolved phases after 1 day. The median pFe_{DS} of all control samples (1 pM, n=12) was subtracted from the pFe_{DS} for each sample. The uptake rate was calculated as:

$$\rho_{dFe} = \frac{[dFe]}{\tau_{Fe_{DS}}} \,, \quad (2)$$

where [dFe] reflects the dFe concentration at 25 m measured by isotope dilution after extraction with Nobias PA-1 resin (Bates & Hawco, 2025).

2.3 Hawaii Ocean Time-series data

Primary production (*in situ* ^{14}C-radiotracer method; Steemann Nielsen, 1952), particulate adenosine-5'-triphosphate (firefly bioluminescence assay; Karl, 1993), particulate carbon, particulate phosphorus, and flow cytometry (Rii et al., 2016) data at Station ALOHA were obtained from the Hawaii Ocean Time-series Data Organization and Graphical System (HOT-DOGS: https://hahana.soest.hawaii.edu/hot/hot-dogs/). Primary productivity measurements were not available for all cruises; for March and August of 2021 and 2022, the 5-year mean (2019-2023) of March and August measurements were used. For pFe sampling at 15 m and 300 m depths, no HOT corresponding samples were available and HOT parameters for these depths were linearly interpolated from samples immediately above and below these depths.

3 Results and Discussion

3.1 Seasonal variability in Fe uptake

We measured iron uptake rates at 25 m on 12 cruises to Station ALOHA in 2021-2023, with good seasonal coverage for spring (MAM, n=4), summer (JJA, n=5), and fall (SON, n=3), but with no experiments conducted during winter. Concurrent measurements of water column dissolved and suspended particulate Fe, as well as sinking particulate Fe from midwater sediment traps, were conducted on these cruises and on 9 additional cruises between December 2020-November 2023 (Bates et al., 2025; Bates & Hawco, 2025). Seasonal variability was observed for all Fe phases measured, with euphotic zone dFe, labile pFe, and lithogenic pFe higher in winter and spring (Fig. 1 and Fig. S1 in Supplement), driven by local island inputs in winter and Asian dust deposition in spring (Bates & Hawco, 2025). Significant interannual

Deleted: both

Deleted: ,

Deleted: ,

Deleted: and

Deleted: also

Deleted: ,

Deleted: as well as

variability was also evident, with large dust-driven peaks in particulate Fe export observed in May 2021 and 2022, but not in 2023, likely reflecting lower dust deposition in 2023 (Fig. S1 in Supplement; Bates et al., 2025). Additionally, anomalously high dFe was found in September 2022, coinciding with a large diazotroph bloom (Foreman et al., 2025).

Bulk iron uptake rates varied ~2.5-fold by month and were, on average, highest in spring (71 ± 11 pM d^{-1}, mean and 1 SD) and lowest in summer and fall (40 ± 15 pM d^{-1} in summer and 41 ± 19 pM d^{-1} in fall; Fig. 1). Uptake rates generally increased with dFe concentration (Fig. 1e), but also appeared to be driven by other factors. Indeed, uptake rates were similar in May for both 2021 and 2023 (79 ± 36 and 80 ± 37 pM d^{-1}, respectively) despite a ~2-fold difference in mean mixed layer dFe concentrations (0.50 ± 0.08 and 0.27 ± 0.02 nM, respectively; Bates & Hawco, 2025). Fe uptake rates were instead correlated with *Prochlorococcus* and picoeukaryote cell counts (R^2 = 0.47 and 0.41, respectively, Fig. 1) and a multiple linear regression model for both populations showed an improved fit with Fe uptake rates (R^2 = 0.89, Fig. 1f, further details in Supplement). From the slope of the multiple linear regression, we can calculate apparent cellular uptake rates of 0.45 amol Fe $cell^{-1}$ d^{-1} for *Prochlorococcus* and 39 amol Fe $cell^{-1}$ d^{-1} for picoeukaryotes. The *Prochlorococcus* rate agrees with previously reported *Prochlorococcus*-specific Fe uptake rates (Lory et al., 2022), while the ~100-fold difference between the two groups is consistent with the ~100-fold difference in group-specific ^{14}C productivity rates (Rii et al., 2016). *Prochlorococcus* and picoeukaryotes together make up the bulk of picophytoplankton biomass and primary production at Station ALOHA (Rii et al., 2016). In contrast, uptake rates did not correlate well with abundances of *Synechococcus* or heterotrophic bacteria (R^2 = 0.09 and 0.15, respectively; Table S1 and Fig. S2 in Supplement). ^{14}C-based primary production was less variable than Fe uptake rates over these cruises (RSD = 0.13 for primary production compared to 0.40 for Fe uptake; Fig. 1g) and did not correlate well with cell abundances (R^2 < 0.1 for *Prochlorococcus*, *Synechococcus*, picoeukaryotes, and heterotrophic bacteria). As a result, our inferred Fe:C uptake ratios showed a similar temporal trend to bulk iron uptake rates (Fig. 1h).

Deleted: b

Deleted: e

Formatted: Superscript

Formatted: Superscript

Formatted: Superscript

Formatted: Superscript

Formatted: Superscript

Deleted:

Formatted: Superscript

Deleted: f

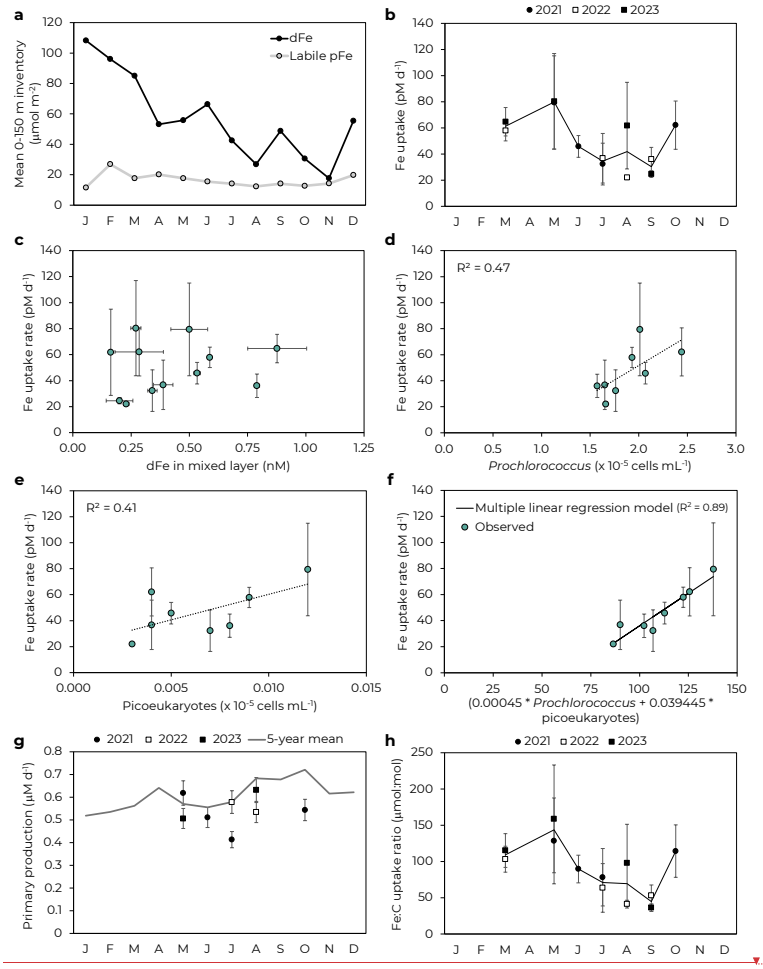

Figure 1: Drivers of Fe uptake. (a) Seasonal variability of mean 0-150 m inventory of dissolved and labile particulate Fe (Bates & Hawco, 2025). (b) Fe uptake rates at 25 m by month. Error bars represent 1 SD of triplicate incubations. Data points without visible error bars have uncertainties smaller than the marker size. Black line follows mean by month. (c) Fe uptake rate as a function of mixed layer dFe concentration. (d) *Prochlorococcus* and (e) picoeukaryotes at 25 m correlate with Fe uptake rates. Note these panels just include data for 2021-2022 for which flow cytometry data is available. (f) Multiple linear regression of Fe uptake rate as a function of *Prochlorococcus* and picoeukaryote abundance. (g) ^{14}C-based primary productivity by month. Line shows mean productivity by month for 2019-2023. (h) Fe:C uptake ratio by month.

Deleted:

Formatted: Centered

Deleted: a… Fe uptake rates at 25 m by month. Error b… [1]

Formatted: Superscript

Deleted: f

Iron uptake rates agreed well with previously reported rates in the subtropical North Pacific. Hawco et al. (2022) found a bulk Fe uptake rate of 48 ± 13 pM d^{-1} for June 2019 at Station ALOHA, in agreement with our summer uptake rate of 40 ± 15 pM d^{-1}. This rate of ~50 pM d^{-1} was determined to be reasonable based on the kinetic constraints of biological Fe' uptake (Hawco et al., 2022). Similar uptake rates were observed for Fe addition experiments at Station ALOHA (43 ± 27 pM d^{-1} for $FeCl_3$, Bundy et al., 2025). The corresponding Fe:C uptake ratios (58 ± 17 and 68 ± 43 µmol:mol for Hawco et al. (2022) and Bundy et al. (2025), respectively) also agreed well with our inferred Fe:C ratios. Price et al. (1994) reported oligotrophic Fe uptake rates south of Hawai'i at 15°N, 152.5°W, with Fe additions of 0.06-2 nM used to calculate a maximum uptake rates based on Michaelis-Menten kinetics. Approximate conversions of their reported data to pM Fe d^{-1} units yield an estimated maximum uptake rate of ~76 pM Fe d^{-1}, close to our maximum observed rate of 80 pM d^{-1} in May 2022 and 2023. The maximum Fe:C uptake ratio (~116 µmol:mol, Price et al., 1994) also fell within 1 SD of our observed Fe:C uptake ratios in May 2022 and 2023 (128 ± 60 and 159 ± 74 µmol:mol, respectively).

3.2 Estimating pFe in biomass using three different approaches

Quantifying the amount of Fe in biomass is challenging, due in part to issues in quantifying living biomass in the ocean generally. Here, we assess three different approaches to calculating particulate Fe in biomass (pFe_{Bio}). First, following the approach by Sofen et al. (2023) to determine biogenic pFe, we use particulate carbon (PC) and particulate phosphorus (PP), which likely include both living cellular and 'dead' organic detrital material, although to different extents. For the final approach, we estimate biotic pFe, or Fe in living biomass, using adenosine-5'-triphosphate (ATP) due to the rapid hydrolysis of ATP following cell death (Holm-Hansen & Booth, 1966). The pFe_{Bio} estimated by these approaches is compared to the suspended pFe_{Labile}, defined using the Berger et al. (2008) labile leach. The Berger et al. (2008) leach was originally developed to estimate labile pFe in a river plume and coastal waters, but subsequent applications in oligotrophic waters have shown that it can effectively solubilize biologically relevant pools of pFe (Rauschenberg & Twining, 2015). Thus, labile pFe represents an approximate maximum for pFe_{Bio}, if there were no additional contributions from the remainder of the labile pFe pool (including authigenic pFe).

For the first approach, pFe_{Bio_PC} was calculated as:

$$pFe_{Bio\_PC} = Fe{:}C \times PC\ , \quad (3)$$

where Fe:C is the molar ratio determined using the bulk iron uptake rates and the HOT primary productivity measurements at 25 m. PFe_{Bio_PP} was calculated as:

$$pFe_{Bio\_PP} = Fe{:}C \times PP \times C{:}P_{Phyto}\ , \quad (4)$$

where $C{:}P_{Phyto}$ is the ratio of C:P of phytoplankton at Station ALOHA. As the C:P of living biomass at Station ALOHA is not well constrained, we estimated $C{:}P_{Phyto}$ based on the mean of previously reported C:P ratios of *Prochlorococcus, Synechococcus,* and picoeukaryotes in the North Pacific Subtropical Gyre (186, 195, and 109 mol:mol, respectively; Lomas

Deleted: biogenic

Deleted: biogenic

Deleted: we use

Deleted: an approach for quantifying living biomass

Deleted: in dead biomass

Deleted: ,

Deleted: which has been shown to capture the biogenic pool

Deleted: nonliving

Deleted: pFe_{Nonliv},

et al., 2021), weighted by the relative depth-integrated (0-125 m) carbon biomass of each group at Station ALOHA (mean: 69%, 3%, and 28%, respectively; Rii et al., 2016), resulting in a C:P_{Phyto} approximation of 165 mol:mol.

The PC and PP approaches consistently overestimated pFe_{Bio}, which almost always exceeded measurements of pFe_{Labile} (Fig. 2). In the mixed layer, both approaches estimated pFe_{Bio} concentrations to be more than double the pFe_{Labile} concentration (mean: 220% and 256% of pFe_{Labile}, respectively). Both approaches continued to overestimate pFe_{Bio} throughout the 150 m euphotic zone, and, in the mesopelagic, reached concentrations equivalent to 78 ± 16% (PC) and 77 ± 23% (PP) of pFe_{Labile} (based on the mean profiles in Fig. 2b). This is likely still an overestimation, as pFe_{Labile} is expected to be dominated by authigenic pFe below the euphotic zone (Sofen et al., 2023).

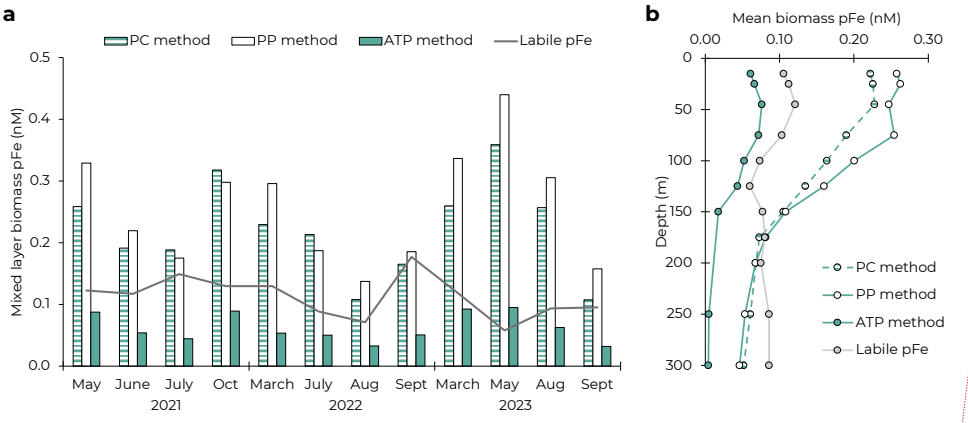

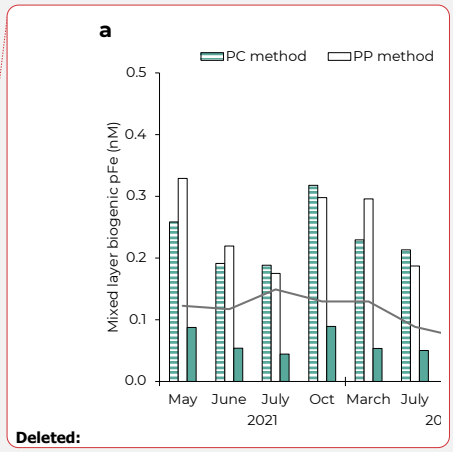

Figure 2: Comparison of three approaches to estimating biomass particulate Fe using PC, PP, and ATP. (a) Average mixed layer concentrations of pFe_{Bio} on the 12 cruises. Grey line shows the mixed layer concentration of pFe_{Labile}, which should represent a maximum potential pFe_{Bio} concentration if there were no authigenic contributions. (b) Mean upper ocean profiles of pFe_{Bio} by the three approaches and pFe_{Labile}.

There are several potential explanations for the overestimation by the PC and PP approaches. First, total PC could include inorganic contributions from calcium carbonate. However, suspended particulate inorganic carbon is very low in oligotrophic gyres (approximately 6% of PC; Gordon, 1971; Hebel & Karl, 2001) and often considered negligible to the total carbon mass balance at Station ALOHA (Gordon, 1971; Karl et al., 2021). The discrepancy may also come from detrital organic matter, including dead cells and fecal pellets, which is estimated to comprise 58-74% of the surface PC pool at Station ALOHA (Henderikx-Freitas et al., 2021; Karl et al., 2022). Unlike organic carbon (as well as N and P), Fe in metalloproteins is not covalently bonded, and so may be released more easily after cell death as cell proteins become denatured. It appears that the Fe:C stoichiometry of this detrital organic carbon is significantly lower than in living cells.

Deleted:
Deleted: biogenic
Deleted: biogenic
Deleted: labile
Deleted: biogenic
Deleted: biogenic
Formatted: Subscript
Deleted: labile

With the PP approach, there is also uncertainty in the C:P of living cells and how this ratio varies over time, which could distort the overestimation of pFe_{Bio}. While the stoichiometries of the different phytoplankton groups are expected to be flexible (Baer et al., 2017; Geider & La Roche, 2002; Karl et al., 2001) and the phytoplankton community composition varies temporally (Pasulka et al., 2013), we expect these complications to have a relatively small impact on our estimation of pFe_{Bio}. Additionally, the calculated $C:P_{Phyto}$ used in Eq. 4 omits a major contribution from heterotrophic bacteria to bulk biomass (Karl et al., 2022) and therefore may overestimate the true C:P of living biomass (Fagerbakke et al., 1996; White et al., 2019). The calculation was repeated using the Redfield C:P of 106 mol:mol (Redfield, 1958), which still regularly overestimated pFe_{Bio} above pFe_{Labile} (Fig. S3 in Supplement). For the mixed layer, we calculated the maximum C:P that would not lead to an overestimation of biogenic pFe (pFe_{Bio} = pFe_{Labile}) to be 80 ± 36 mol:mol (average and 1 SD across cruises). This assumes the entire labile pFe pool is biogenic, which would conflict with previous conclusions about the importance of authigenic pFe (Sofen et al., 2023), requiring C:P to decrease further. Importantly, moderate phosphate depletion at Station ALOHA indicates that C:P in cells should exceed the 106:1 Redfield ratio (Björkman et al., 2000; Karl et al., 2001). Thus, we conclude that the overestimations of pFe_{Bio} by Eq. 3 and 4 are due to nonliving contributions to both the PC and PP inventories.

To avoid the contributions of nonliving organic matter to the PC and PP pools, we used particulate ATP as an estimate of living biomass. An essential molecule for energy generation in all organisms, ATP is turned over quickly via rapid release following cell death and does not easily adsorb to other particulate matter (Holm-Hansen & Booth, 1966). ATP is not commonly measured in the ocean, but has been measured regularly at Station ALOHA since 1989 (Karl et al., 2022), providing a unique method for estimating Fe in living biomass. Previous work using ATP suggests only 26-42% of the surface particulate carbon pool at Station ALOHA is comprised of living biomass (Henderikx-Freitas et al., 2021; Karl et al., 2022). Applying ATP as a biomass indicator restricts the pFe_{Bio} estimate to the Fe quotas in living cells, excluding any biologically-derived Fe in dead cells or biogenic exudates. We calculated pFe_{Bio_ATP} as:

$$pFe_{Bio\_ATP} = Fe{:}C \times \left(\frac{ATP \times 250}{12.01}\right), \quad (5)$$

where 250 represents the ratio of living C to ATP in g g^{-1} (Karl, 1980). One important limitation for this approach is that the C:ATP ratio must be well constrained. At Station ALOHA, C:ATP has been reported to fall between 250-400 g g^{-1} (Christian & Karl, 1994; Karl, 1980). Recent work based on shipboard experiments and *Prochlorococcus* measurements supports the use of a 250 C:ATP ratio at Station ALOHA (Karl et al., 2022), in agreement with a variety of other field and laboratory studies of marine organisms (Bochdansky et al., 2021; Holm-Hansen, 1970, 1973). Additionally, there is some uncertainty in the influence of heterotrophic bacteria on the C:ATP ratio, which has been reported for heterotrophic bacteria at ~100 g g^{-1} (Hewes et al., 1990).

The ATP approach produced pFe_{Bio_ATP} values that were consistently less than pFe_{Labile}, both in the mixed layer and at depth, thereby satisfying our mass balance constraint on pFe_{Bio}. Across the 12 cruises where Fe uptake data were

Deleted: not represent

Formatted: Subscript

Formatted: Subscript

Deleted: R

Formatted: Superscript

available, pFe_{Bio_ATP} averaged 61 ± 37% of pFe_{Labile} in the mixed layer (Fig. 2a). Below 150 m, pFe_{Bio_ATP} comprised <15% of pFe_{Labile} (Fig. 2b).

For all three approaches, there are also limitations in estimating pFe_{Bio} from the calculation and application of the Fe:C uptake ratio. First, there is uncertainty in the Fe:C uptake ratios based on variability in the replicate Fe uptake incubations (error bars in Fig. 1h). The mean replicate RSD from this timeseries was 30% or 27 µmol:mol. Additionally, our method of determining Fe:C is based on bulk uptake rates and includes an assumption that the turnover time of the Fe_{DS} addition is equivalent to the turnover time of the entire dFe pool (Hawco et al., 2022). The long pre-incubation time allows for the added Fe to bind with strong Fe ligands routinely observed at Station ALOHA (Bundy et al., 2018; Fitzsimmons et al., 2015; Rue & Bruland, 1995), which makes this approximation more reasonable. In this study, we also added a control incubation to account for production of pFe from colloidal aggregation of Fe oxide precipitation, which yield a median uptake rate of 12.5 pM d^{-1} (note that this does not account for 'heterogeneous' scavenging or aggregation of dFe onto pre-existing particles). Finally, to estimate pFe_{Bio} throughout the upper water column, the Fe:C uptake ratio at 25 m was assumed to reflect the Fe:C quota of biota regardless of depth, which is a problematic simplification. This ratio likely changes with depth due to changes in dFe concentration, community composition (Twining et al., 2021), and increased Fe quotas under light limitation (Hawco et al., 2022; Hogle et al., 2022; Raven, 1990). Despite these known mechanisms, direct comparisons of phytoplankton Fe quotas between the surface mixed layer and deep chlorophyll maximum (DCM) in the subtropical North Atlantic has not necessarily pointed to meaningful differences in Fe:C (Sofen et al., 2023).

3.3 Estimating authigenic + detrital pFe

Overall, the ATP approach provides the most reasonable biotic pFe estimates of the three approaches assessed, and hereafter pFe_{Bio_ATP} is referred to as pFe_{Bio}. We therefore used this method to further estimate the remainder of the labile pFe pool ($pFe_{Auth+Det}$) by subtraction, operationally defined by the equation:

$$pFe_{Auth+Det} = pFe_{Labile} - pFe_{Bio} \quad (6)$$

For samples where the pFe_{Bio} exceeded pFe_{Labile} (n=12, 12% of samples), $pFe_{Auth+Det}$ was set to 0. As in Sofen et al. (2023), pFe_{Bio} samples were permitted to be up to 125% of pFe_{Labile} due the heterogeneity of oceanic particles and considering measurement uncertainties. Samples where pFe_{Bio} was greater than 125% of pFe_{Labile} (n=7, 7% of samples) were set to 1.25 times pFe_{Labile}. The majority of these samples were in March 2022 and May 2023, all within the euphotic zone.

There has been considerable interest recently in quantifying the authigenic pFe pool, which is likely generated by different mechanisms than pFe_{Bio} and may be exported with different efficiencies. While the ATP approach offers our most reasonable estimate of the authigenic pFe pool due to the overestimations observed by the PC and PP approaches, it is important to consider that using this definition likely includes some particulate Fe outside of authigenic Fe oxyhydroxides precipitated *in situ* from dFe. First, this approach may include non-mineral Fe in or adsorbed to nonliving organic particles, such as in detrital organic matter, shown above to be a significant portion of the particulate C and P pools. Additionally,

Deleted: f

Deleted: nonliving labile

Deleted: pFe_{Bio}

Formatted: Subscript

Formatted: Subscript

Deleted: Nonliv

Formatted: Not Superscript/ Subscript

Deleted: _ATP

Deleted: Nonliv

Formatted: Not Superscript/ Subscript

Deleted: includes

exogenous lithogenic particles from the atmosphere or advected from the Hawaiian Islands also contain a significant fraction of chemically labile Fe that is dissolved by the Berger et al. (2008) leach (~5-20% depending on the source; Shelley et al., 2018). Dust-derived contributions to the pFe_{Labile} pool would be seasonally variable, with peak dust deposition expected in spring (Parrington et al., 1983; Prospero et al., 2003). While the particles might contain amorphous Fe oxyhydroxides that are chemically identical to authigenic pFe, they were not formed *in situ* and so are not strictly authigenic. Regardless, the ATP approach allows for the separation of Fe in living biomass to understand how the behavior of this pool differs from the remainder of the pFe_{Labile} pool.

3.4 Biotic and authigenic + detrital particulate Fe distributions at Station ALOHA

The derived profiles of pFe_{Bio} and $pFe_{Auth+Det}$ differed substantially, with mean pFe_{Bio} higher in the upper 125 m and $pFe_{Auth+Det}$ dominating below 125 m (Fig. 3). The mean pFe_{Labile} profile across the 12 cruises was highest (0.10-0.12 nM) in the upper euphotic zone (0-75 m), lowest in the DCM (100-125 m), and relatively consistent with depth from 150-300 m at 0.07-0.09 nM. Particulate Fe_{Bio} was high throughout the upper euphotic zone (≥ 0.05 nM in the upper 100 m), with no minimum in the DCM. Below 150 m, pFe_{Bio} was < 0.01 nM in the upper mesopelagic, reflecting the steep decline in ATP. The structure of the average pFe_{Bio} profile with depth aligns with upper ocean profiles of *Prochlorococcus* and other phytoplankton at Station ALOHA (Campbell & Vaulot, 1993; van den Engh et al., 2017). In contrast, $pFe_{Auth+Det}$ was slightly elevated in the surface mixed layer (0.05 nM on average in the upper 45 m), with a local minimum near the DCM, and increased into the upper mesopelagic. A local minimum in authigenic pFe at the DCM was observed previously (Sofen et al., 2023), attributed to either the dissolution of authigenic pFe with the dFe minimum, or to increased export efficiency of authigenic pFe in the subsurface. As in the North Atlantic, observations of colloidal Fe at Station ALOHA have also shown a minima around the DCM (Fitzsimmons et al., 2015), as does pFe_{Lith}. From these mean profiles, pFe_{Labile} is majority biotic in the euphotic zone (59-72% in the upper 125 m), and majority authigenic + detrital below the DCM (>90% at 250-300 m; Fig. 3b). Refractory pFe is chemically inert and should only be affected by particle aggregation, disaggregation, and export processes. Based on the similarity between $pFe_{Auth+Det}$ and pFe_{Lith}, we suggest that the $pFe_{Auth+Det}$ profile is also primarily driven by these processes.

Deleted: ing
Deleted: , nonliving
Deleted: Biogenic
Deleted: nonliving
Deleted: Nonliv
Formatted: Not Superscript/ Subscript
Deleted: Nonliv
Formatted: Not Superscript/ Subscript
Deleted: Nonliv
Formatted: Not Superscript/ Subscript
Deleted: pFeNonliv
Formatted: Not Superscript/ Subscript
Deleted: biogenic
Deleted: nonliving
Deleted: Nonliv
Deleted: which should be chemically inert,
Deleted: Nonliv
Formatted: Not Superscript/ Subscript
Formatted: Not Superscript/ Subscript
Deleted: particle aggregation and export processes

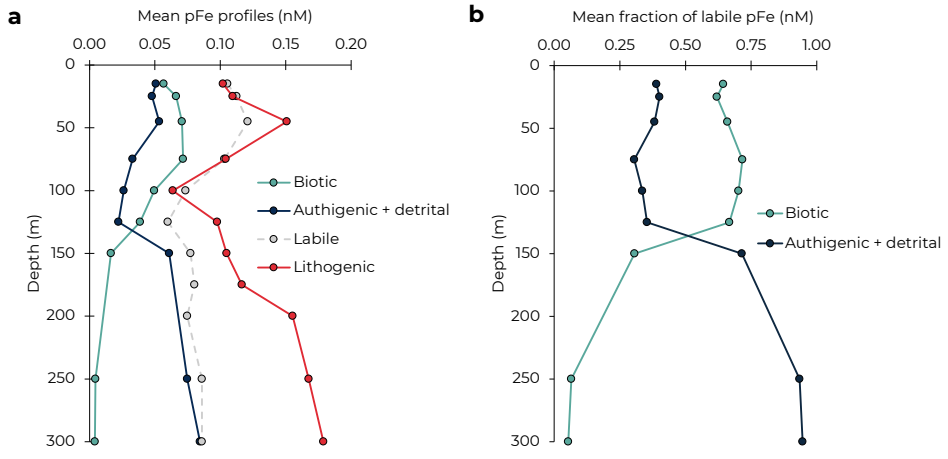

Figure 3: Mean profiles of particulate Fe phases (a). The fraction of labile pFe comprised of biotic and authigenic + detrital pFe, averaged across cruises (b).

The seasonal cycle of pFe_{Bio} in the mixed layer was similar to bulk Fe uptake rates, with generally higher concentrations in the spring (ranging 0.06-0.09 nM) and lower concentrations in summer (ranging 0.04-0.06 nM, Fig. 4). PFe_{Bio} also appears to be driven by *Prochlorococcus* and picoeukaryotes abundances (R^2 = 0.63 and 0.14, respectively). The correlation between picoeukaryotes and pFe_{Bio} is marred by data from October 2021, when *Prochlorococcus* was 30% greater than the mean abundance and peak pFe_{Bio} occurred.

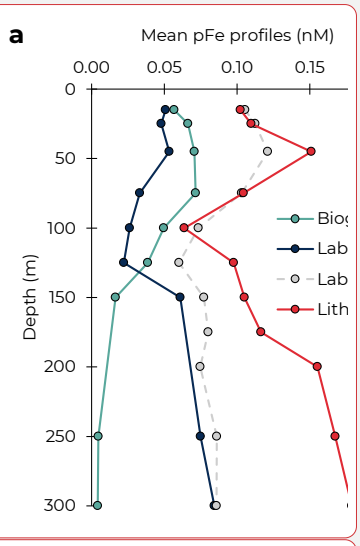

Deleted:

Deleted: biogenic

Deleted: nonliving

Deleted: an outlier in

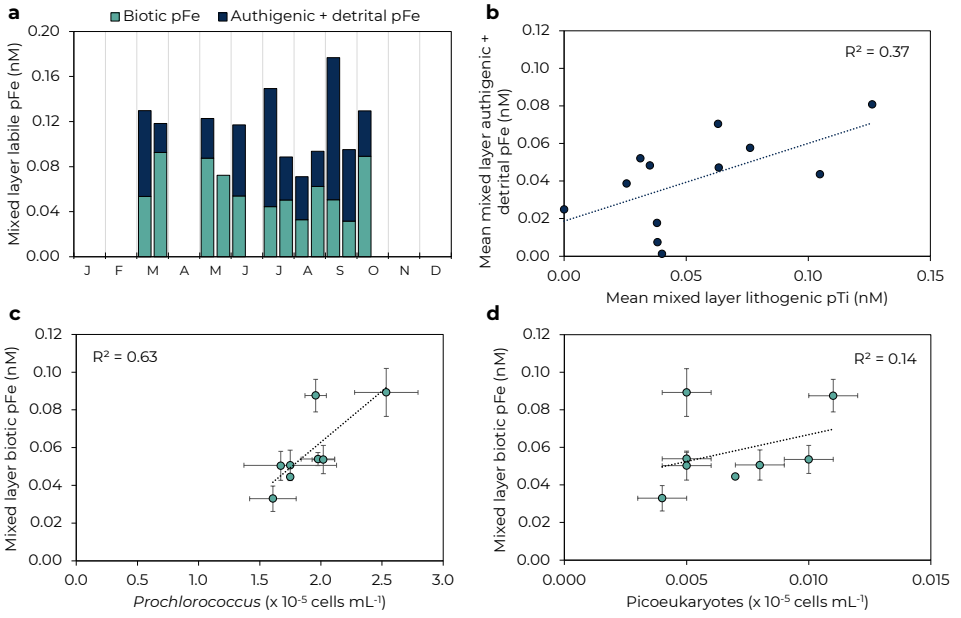

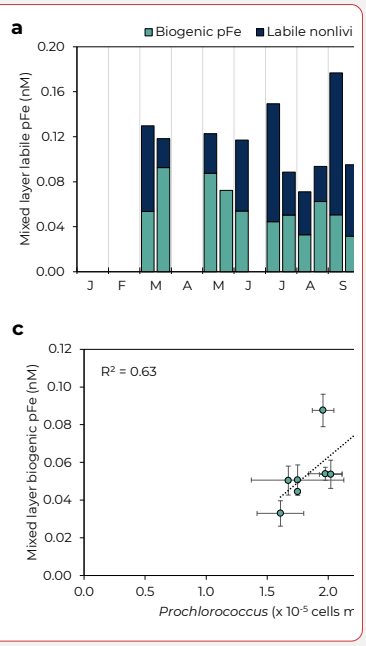

Figure 4: Seasonal changes in mixed layer biotic and authigenic + detrital labile particulate Fe. (a) Biotic (green) and authigenic + detrital (navy) pFe by month. (b) Correlation of mean lithogenic particulate Ti and authigenic + detrital pFe in the mixed layer. (c) *Prochlorococcus* and (d) picoeukaryotes in the mixed layer correlate with mixed layer biogenic pFe. Error bars represent 1 SD of samples in the mixed layer. Note panels c-d just include data for 2021-2022; flow cytometry data is not available for 2023.

Mean $pFe_{Auth+Det}$ in the mixed layer overall varied over a larger range than pFe_{Bio}, from 0–0.13 nM, but with no clear seasonal pattern. Mixed layer $pFe_{Auth+Det}$ was highest in July 2021 and September 2022 and lowest in March and May 2023. A weak positive correlation with lithogenic particulate Ti at 25 m (R^2 = 0.31, Fig. 4b) suggests input of lithogenic material may play a role in hosting authigenic Fe oxyhydroxides, perhaps via scavenging and/or colloidal aggregation, but this correlation could also be explained by lateral advection of Ti-rich basaltic material containing Fe oxyhydroxides. Authigenic + detrital pFe was not well correlated with any major phytoplankton groups (R^2 = 0.04, 0.12, and 0.01 for *Prochlorococcus*, *Synechococcus*, and picoeukaryotes, respectively; Table S3 in Supplement), suggesting that variations of $pFe_{Auth+Det}$ are not primarily driven by dead biomass or extracellular Fe precipitates. The concentration of colloidal Fe is thought to be important in driving production of authigenic pFe minerals (Kunde et al., 2019; Tagliabue et al., 2023). While colloidal Fe was not measured during our timeseries, the colloidal fraction has been shown to drive dFe variability at Station ALOHA (comprising 64% ± 18% of dFe pool; Bergquist et al., 2007; Fitzsimmons et al., 2015; Wu et al., 2001) and so

Deleted:
Deleted: biogenic
Deleted: nonliving
Deleted: Biogenic
Deleted: nonliving
Deleted: labile
Deleted: at 25 m
Deleted: Nonliv
Formatted: Not Superscript/ Subscript
Deleted: Nonliv
Formatted: Not Superscript/ Subscript
Deleted: Nonliving labile
Deleted: Nonliv
Formatted: Not Superscript/ Subscript

colloidal-driven production should be traceable by dFe. However, mixed layer dFe and $pFe_{Auth+Det}$ were not strongly correlated (R^2 = 0.15), suggesting dFe variability (and thus colloidal Fe variability) is not the primary driver of $pFe_{Auth+Det}$ variability.

Deleted: Nonliv

Formatted: Not Superscript/ Subscript

Deleted: Nonliv

Formatted: Not Superscript/ Subscript

3.5 Comparison to the North Atlantic Subtropical Gyre

As one of the only other open ocean sites with seasonally resolved Fe data, the Bermuda Atlantic Time-series Study (BATS) site in the subtropical North Atlantic serves as a natural comparison to Station ALOHA. While both sites are oligotrophic with similar annual net community production (Emerson, 2014), the BATS site is expected to receive an order of magnitude more annual lithogenic dust deposition (Hayes et al., 2017; Kok et al., 2021), indicating the potential for major differences in Fe cycling. Fortunately, the Fe cycle at BATS has been extensively explored as part of the recent 'BAIT' project (Sedwick et al., 2023; Sofen et al., 2023; Tagliabue et al., 2023). A comparison of Fe profiles across seasons highlights the similarities and differences between the sites (Fig. 5). At both sites, dissolved Fe was present at a similar magnitude, with a similar variability across the seasonal cycle. Mean dFe concentrations in the upper 100 m ranged from 0.28 nM in spring to 0.67 nM in fall at BATS (Sedwick et al., 2023) and from 0.23 nM in fall to 0.64 nM in winter at Station ALOHA (Bates & Hawco, 2025). As expected, pFe_{Lith} was notably higher at BATS, particularly in August (> 1 nM in the surface, Fig. 5e) when Saharan dust deposition was highest (Sedwick et al., 2023; Sofen et al., 2023). The pFe_{Labile} pools were similar between the sites, apart from notably higher concentrations in the upper 50 m at BATS in summer and fall (Fig. 5h-i).

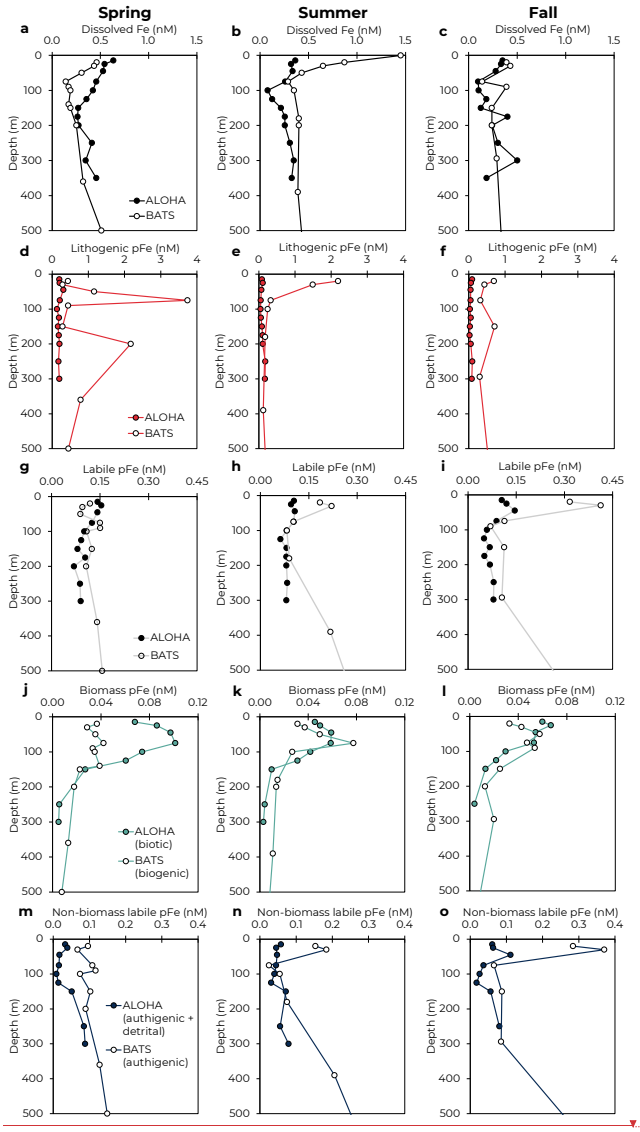
Spring
Summer
Fall
Dissolved Fe (nM)
Lithogenic pFe (nM)
Labile pFe (nM)
Biomass pFe (nM)
Non-biomass labile pFe (nM)
Depth (m)
ALOHA
BATS
ALOHA (biotic)
BATS (biogenic)
ALOHA (authigenic + detrital)
BATS (authigenic)

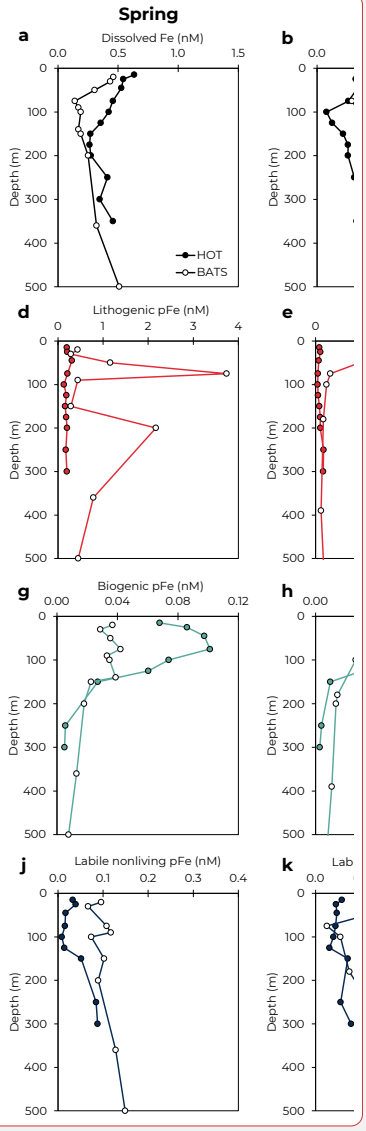
Spring
Dissolved Fe (nM)
Lithogenic pFe (nM)
Biogenic pFe (nM)
Labile nonliving pFe (nM)
Depth (m)
HOT
BATS

Deleted:

Figure 5: Comparison of seasonal Fe dynamics between Station ALOHA (North Pacific Subtropical Gyre; filled) and BATS (North Atlantic Subtropical Gyre; unfilled). Mean profiles of dissolved Fe (a-c), lithogenic pFe (d-f), labile pFe (g-i), biotic or biogenic pFe (j-l), and authigenic or authigenic + detrital pFe (m-o) in the upper 500 m are shown for spring, summer, and fall. Winter not shown due to little to no sampling coverage for most parameters. BATS data from Sedwick et al. (2023) and Sofen et al. (2023).

Within the labile pFe pool, the contributions of biotic and authigenic pFe differed substantially between the sites. At BATS, pFe_{Bio} was consistently lower than authigenic pFe, with the pFe_{Labile} pool ranging 26-36% biogenic by season above the DCM (Sofen et al., 2023). In contrast, pFe_{Bio} contributions at Station ALOHA were higher, comprising 47-84% of pFe_{Labile} above the DCM by season. Overall, pFe_{Bio} concentrations were similar between the sites, with seasonally averaged concentrations in the upper 100 m ranging 0.03-0.10 nM at Station ALOHA and 0.03-0.08 nM at BATS (Fig. 5j-l), in agreement with global estimates for biotic iron pools (Boyd et al., 2015; Sofen et al., 2023). Note that the methods of estimating pFe_{Bio} differ between the two sites. Sofen et al. (2023) estimated pFe_{Bio} using Eq. 4 and cellular Fe quotas of eukaryotes determined by synchrotron X-ray fluorescence. This approach, using labile particulate phosphorus, includes detrital organic material as part of pFe_{Bio} and assumes Fe quotas from living, eukaryotic phytoplankton cells are representative of the entire microbial pool (Sofen et al., 2023). Given the much higher concentration of pFe_{Labile} at BATS, the possible overestimation of pFe_{Bio}, as shown here for Station ALOHA, is less impactful. Regardless, the inclusion of detrital organic material in the pFe_{Bio} estimates at BATS would suggest that biotic pFe in living cells would be comparatively lower than at Station ALOHA, which may be due to differences in phytoplankton community composition or biomass. While the two sites have overall similar magnitudes of phytoplankton biomass (Selph et al., 2022), BATS shows significantly more variability in *Prochlorococcus* over the seasonal cycle, typically only reaching the levels observed at Station ALOHA during spring blooms (Malmstrom et al., 2010). Despite differences in operationally defining the remainder of the labile pool, such as the inclusion of detrital material in the authigenic pool in our methods, much higher authigenic pFe is evident at BATS, particularly in the surface mixed layer (Fig. 5m-o). Increased authigenic pFe at BATS could be due, in part, to the increased pFe_{Lith}. Lithogenic particles scavenge colloidal Fe, with scavenging expected to increase with higher Fe (Boyd et al., 2010; Ye & Völker, 2017). Additionally, pFe_{Lith} may also trace input of exogenous labile pFe from dust, which would be counted in the authigenic pFe pool. Similar to our analysis at Station ALOHA, the higher deposition of lithogenic dust at BATS could drive greater *authigenic* pFe formation, or greater contributions of *exogenous* labile pFe, which does not fully integrate with the dFe pool. This distinction has important implications for the residence time of Fe in the ocean, but future research is needed to separate these possibilities conclusively.

4 Conclusions

Understanding the composition of the labile particulate Fe pool in the upper ocean is essential for unraveling the complexities of marine Fe cycling. This study highlights biotic uptake by *Prochlorococcus* and other phytoplankton as drivers of the pFe_{Bio} pool. The $pFe_{Auth+Det}$ pool, potentially including contributions from detrital organic matter and dust in

Deleted: HOT

Deleted: biogenic

Deleted: , and labile nonliving pFe (g-l)

Deleted: , where pFe_{Auth} is used here labeled as pFe_{Nonliv}

Deleted: biogenic

Deleted: nonliving

Deleted: the

Deleted: $_{Nonliv}$

Deleted: HOT

Deleted: 5g-i

Deleted: Additionally, BATS and Station ALOHA have similar magnitudes of phytoplankton biomass (Selph et al., 2022), which has a large influence on pFe_{Bio} (Fig. 4), although community composition varies somewhat between the sites (DuRand et al., 2001; Pasulka et al., 2013). …

Deleted: eukaryotic

Formatted: Subscript

Deleted: M

Deleted: pFe_{Nonliv}

Deleted: 5j-l

Deleted: $_{Nonliv}$

Deleted: pFe_{Nonliv}

Deleted: $_{Nonliv}$

Formatted: Not Superscript/ Subscript

addition to authigenic minerals, instead appeared to be correlated with lithogenic material. This relationship suggests that $pFe_{Auth+Det}$ may be driven by either scavenging and the precipitation of Fe oxides coatings onto lithogenic material or by direct contributions from dust. Clearly, $pFe_{Auth+Det}$ is an important contributor to the pFe_{Labile} pool at Station ALOHA, comprising ~40% in the euphotic zone and >90% below the euphotic zone. As dFe and pFe_{Bio} are transferred into the $pFe_{Auth+Det}$ pool, potentially via authigenic mineral formation, more efficient recycling of pFe_{Bio} may be necessary to meet biotic Fe demand. Indeed, the greater portion of pFe_{Bio} at Station ALOHA compared to the North Atlantic may be key to sustaining high rates of Fe recycling previously reported for the North Pacific Subtropical Gyre. However, the actual composition of the $pFe_{Auth+Det}$ pool remains elusive. Direct chemical and mineralogical characterization of the operationally-defined $pFe_{Auth+Det}$ pool is needed to assess its reactivity, bioavailability, and origin. Continued investigation into the composition and transformations of $pFe_{Auth+Det}$ is needed to further our understanding of its role in marine Fe cycling.

Deleted: Nonliv
Formatted: Not Superscript/ Subscript
Deleted: Nonliv
Formatted: Not Superscript/ Subscript
Deleted: Nonliv
Formatted: Not Superscript/ Subscript
Deleted: Nonliv
Formatted: Not Superscript/ Subscript
Deleted: Nonliv
Formatted: Not Superscript/ Subscript
Deleted: Nonliv
Formatted: Not Superscript/ Subscript

Data availability

Fe uptake data are available through the Biological and Chemical Oceanography Data Management Office (BCO-DMO) at https://doi.org/10.26008/1912/bco-dmo.994200.1 (Hawco & Bates, 2026). Dissolved, labile particulate, and recalcitrant particulate Fe data are also available through BCO-DMO (Hawco & Bates, 2025a, 2025b, 2025c) at https://doi.org/10.26008/1912/bco-dmo.962986.2, https://doi.org/10.26008/1912/bco-dmo.962966.1, and https://doi.org/10.26008/1912/bco-dmo.962821.1. Hawaii Ocean Time-series data were obtained via the Hawaii Ocean Time-series HOT-DOGS application; University of Hawai'i at Mānoa; National Science Foundation award #2241005 (HOT-DOGS, 2025).

Formatted: Left
Deleted: is
Deleted: on
Deleted: -
Deleted: -
Deleted: -
Deleted: Fe uptake data has been submitted to the Biological and Chemical Oceanography Data Management Office (BCO-DMO). …

Author contributions

NJH and ESB conceptualized the study. ESB performed the experiments and analyzed the samples. Both authors analyzed the data and wrote the paper.

Competing interests

The authors declare that they have no conflict of interest.

Acknowledgements

The authors thank the Hawaii Ocean Time-series team for their assistance throughout the field campaign, particularly Angelicque White for accommodating this work as part of the HOT cruises. We also thank the captains, crews, and marine

technicians aboard the R/V *Kilo Moana*. We thank Seth John and Shun-Chung Yang for assistance with MC-ICP-MS analysis.

Financial support

This work was supported by National Science Foundation award OCE-2022969 to NJH and Simons Foundation Grants 10686 and 924096 to NJH. ESB was also supported by a graduate fellowship from the Uehiro Center for the Advancement of Oceanography.

References

Baer, S. E., Lomas, M. W., Terpis, K. X., Mouginot, C., and Martiny, A. C.: Stoichiometry of *Prochlorococcus, Synechococcus* , and small eukaryotic populations in the western North Atlantic Ocean, Environmental Microbiology, 19, 1568–1583, https://doi.org/10.1111/1462-2920.13672, 2017.

Bates, E. S. and Hawco, N. J.: Dissolved Iron Seasonal Cycle and Residence Time in the North Pacific Subtropical Gyre, Geophysical Research Letters, 52, e2025GL118095, https://doi.org/10.1029/2025GL118095, 2025.

Bates, E. S., White, A. E., and Hawco, N. J.: Variability and Export Timescales of Upper Ocean Particulate Trace Metals in the North Pacific Subtropical Gyre, Global Biogeochemical Cycles, 39, https://doi.org/10.1029/2025GB008657, 2025.

Berger, C. J. M., Lippiatt, S. M., Lawrence, M. G., and Bruland, K. W.: Application of a chemical leach technique for estimating labile particulate aluminum, iron, and manganese in the Columbia River plume and coastal waters off Oregon and Washington, Journal of Geophysical Research: Oceans, 113, https://doi.org/10.1029/2007JC004703, 2008.

Bergquist, B. A., Wu, J., and Boyle, E. A.: Variability in oceanic dissolved iron is dominated by the colloidal fraction, Geochimica et Cosmochimica Acta, 71, 2960–2974, https://doi.org/10.1016/j.gca.2007.03.013, 2007.

Björkman, K., Thomson-Bulldis, A. L., and Karl, D. M.: Phosphorus dynamics in the North Pacific subtropical gyre, Aquatic Microbial Ecology, 22, 185–198, https://doi.org/10.3354/ame022185, 2000.

Black, E. E., Kienast, S. S., Lemaitre, N., Lam, P. J., Anderson, R. F., Planquette, H., Planchon, F., and Buesseler, K. O.: Ironing Out Fe Residence Time in the Dynamic Upper Ocean, Global Biogeochem. Cycles, 34, https://doi.org/10.1029/2020GB006592, 2020.

Bochdansky, A. B., Stouffer, A. N., and Washington, N. N.: Adenosine triphosphate (ATP) as a metric of microbial biomass in aquatic systems: new simplified protocols, laboratory validation, and a reflection on data from the literature, Limnology and Oceanography: Methods, 19, 115–131, https://doi.org/10.1002/lom3.10409, 2021.

Boyd, P. W., Ibisanmi, E., Sander, S. G., Hunter, K. A., and Jackson, G. A.: Remineralization of upper ocean particles: Implications for iron biogeochemistry, Limnology and Oceanography, 55, 1271–1288, https://doi.org/10.4319/lo.2010.55.3.1271, 2010.

Boyd, P. W., Strzepek, R. F., Ellwood, M. J., Hutchins, D. A., Nodder, S. D., Twining, B. S., and Wilhelm, S. W.: Why are biotic iron pools uniform across high- and low-iron pelagic ecosystems?, Global Biogeochemical Cycles, 29, 1028–1043, https://doi.org/10.1002/2014GB005014, 2015.

Boyd, P. W., Ellwood, M. J., Tagliabue, A., and Twining, B. S.: Biotic and abiotic retention, recycling and remineralization of metals in the ocean, Nature Geosci, 10, 167–173, https://doi.org/10.1038/ngeo2876, 2017.

Bressac, M., Guieu, C., Ellwood, M. J., Tagliabue, A., Wagener, T., Laurenceau-Cornec, E. C., Whitby, H., Sarthou, G., and Boyd, P. W.: Resupply of mesopelagic dissolved iron controlled by particulate iron composition, Nat. Geosci., 12, 995–1000, https://doi.org/10.1038/s41561-019-0476-6, 2019.

Bundy, R. M., Boiteau, R. M., McLean, C., Turk-Kubo, K. A., McIlvin, M. R., Saito, M. A., Van Mooy, B. A. S., and Repeta, D. J.: Distinct Siderophores Contribute to Iron Cycling in the Mesopelagic at Station ALOHA, Frontiers in Marine Science, 5, https://doi.org/10.3389/fmars.2018.00061, 2018.

Bundy, R. M., Manck, L. E., Repeta, D. J., Church, M. J., Hawco, N. J., Boiteau, R. M., Park, J., DeLong, E. F., and Saito, M. A.: Patterns of siderophore production and utilization at Station ALOHA from the surface to mesopelagic waters, Limnology and Oceanography, 70, 128–145, https://doi.org/10.1002/lno.12746, 2025.

Campbell, L. and Vaulot, D.: Photosynthetic picoplankton community structure in the subtropical North Pacific Ocean near Hawaii (station ALOHA), Deep Sea Research Part I: Oceanographic Research Papers, 40, 2043–2060, https://doi.org/10.1016/0967-0637(93)90044-4, 1993.

Christian, J. R. and Karl, D. M.: Microbial community structure at the U.S.-Joint Global Ocean Flux Study Station ALOHA: Inverse methods for estimating biochemical indicator ratios, Journal of Geophysical Research: Oceans, 99, 14269–14276, https://doi.org/10.1029/94JC00681, 1994.

Emerson, S.: Annual net community production and the biological carbon flux in the ocean, Global Biogeochemical Cycles, 28, 14–28, https://doi.org/10.1002/2013GB004680, 2014.

van den Engh, G. J., Doggett, J. K., Thompson, A. W., Doblin, M. A., Gimpel, C. N. G., and Karl, D. M.: Dynamics of Prochlorococcus and Synechococcus at Station ALOHA Revealed through Flow Cytometry and High-Resolution Vertical Sampling, Front. Mar. Sci., 4, https://doi.org/10.3389/fmars.2017.00359, 2017.

Fagerbakke, K., Heldal, M., and Norland, S.: Content of carbon, nitrogen, oxygen, sulfur and phosphorus in native aquatic and cultured bacteria, Aquat. Microb. Ecol., 10, 15–27, https://doi.org/10.3354/ame010015, 1996.

Fitzsimmons, J. N., Hayes, C. T., Al-Subiai, S. N., Zhang, R., Morton, P. L., Weisend, R. E., Ascani, F., and Boyle, E. A.: Daily to decadal variability of size-fractionated iron and iron-binding ligands at the Hawaii Ocean Time-series Station ALOHA, Geochimica et Cosmochimica Acta, 171, 303–324, https://doi.org/10.1016/j.gca.2015.08.012, 2015.

Deleted: DuRand, M. D., Olson, R. J., and Chisholm, S. W.: Phytoplankton population dynamics at the Bermuda Atlantic Time-series → station in the Sargasso Sea, Deep Sea Research Part II: Topical Studies in Oceanography, 48, 1983–2003, → https://doi.org/10.1016/S0967-0645(00)00166-1, 2001.¶

Formatted: Font: Not Bold

Formatted: Font: Not Bold

Foreman, R. K., Barone, B., Grabowski, E., Björkman, K. M., Freitas, F. H., Garcia, C., Manck, L. E., White, A. E., Church, M. J., and Karl, D. M.: Biogeochemical anatomy and ecosystem dynamics of a large phytoplankton bloom north of the Hawaiian Islands, Progress in Oceanography, 103620, https://doi.org/10.1016/j.pocean.2025.103620, 2025.

Geider, R. and La Roche, J.: Redfield revisited: variability of C:N:P in marine microalgae and its biochemical basis, European Journal of Phycology, 37, 1–17, https://doi.org/10.1017/S0967026201003456, 2002.

Goldberg, E. D.: Marine Geochemistry 1. Chemical Scavengers of the Sea, The Journal of Geology, 62, 249–265, https://doi.org/10.1086/626161, 1954.

Gordon, D. C.: Distribution of particulate organic carbon and nitrogen at an oceanic station in the central Pacific, Deep Sea Research and Oceanographic Abstracts, 18, 1127–1134, https://doi.org/10.1016/0011-7471(71)90098-2, 1971.

Gunnars, A., Blomqvist, S., Johansson, P., and Andersson, C.: Formation of Fe(III) oxyhydroxide colloids in freshwater and brackish seawater, with incorporation of phosphate and calcium, Geochimica et Cosmochimica Acta, 66, 745–758, https://doi.org/10.1016/S0016-7037(01)00818-3, 2002.

Hawco, N. J. and Bates, E. S.: Sediment trap metal fluxes from Hawaii Ocean Timeseries (HOT) R/V Kilo Moana cruises at station ALOHA, North Pacific Subtropical Gyre, from December 2020 to November 2023, BCO-DMO [data set], https://doi.org/10.26008/1912/BCO-DMO.962821.1, 2025a.

Hawco, N. J. and Bates, E. S.: Water column dissolved and total dissolvable metal concentrations from Hawaii Ocean Timeseries (HOT) R/V Kilo Moana cruises at station ALOHA, North Pacific Subtropical Gyre, from December 2020 to November 2023, BCO-DMO [data set], https://doi.org/10.26008/1912/BCO-DMO.962986.1, 2025b.

Hawco, N. J. and Bates, E. S.: Water column particulate metals from Hawaii Ocean Timeseries (HOT) R/V Kilo Moana cruises at station ALOHA, North Pacific Subtropical Gyre, from December 2020 to November 2023, BCO-DMO [data set], https://doi.org/10.26008/1912/BCO-DMO.962966.1, 2025c.

Hawco, N. J. and Bates, E. S.: Iron uptake rates from Hawaii Ocean Time-series (HOT) cruises on R/V Kilo Moana at Station ALOHA in the North Pacific Subtropical Gyre from May 2021 to September 2023, BCO-DMO [data set], https://doi.org/10.26008/1912/bco-dmo.994200.1, 2026.

Hawco, N. J., Yang, S.-C., Pinedo-González, P., Black, E. E., Kenyon, J., Ferrón, S., Bian, X., and John, S. G.: Recycling of dissolved iron in the North Pacific Subtropical Gyre, Limnology and Oceanography, 67, 2448–2465, https://doi.org/10.1002/lno.12212, 2022.

Hayes, C. T., Rosen, J., McGee, D., and Boyle, E. A.: Thorium distributions in high- and low-dust regions and the significance for iron supply, Global Biogeochemical Cycles, 31, 328–347, https://doi.org/10.1002/2016GB005511, 2017.

Hebel, D. V. and Karl, D. M.: Seasonal, interannual and decadal variations in particulate matter concentrations and composition in the subtropical North Pacific Ocean, Deep Sea Research Part II: Topical Studies in Oceanography, 48, 1669–1695, https://doi.org/10.1016/S0967-0645(00)00155-7, 2001.

Formatted: Default Paragraph Font, English (UK)

Henderikx-Freitas, F., Karl, D. M., Björkman, K. M., and White, A. E.: Constraining growth rates and the ratio of living to nonliving particulate carbon using beam attenuation and adenosine-5′-triphosphate at Station ALOHA, Limnology and Oceanography Letters, 6, 243–252, https://doi.org/10.1002/lol2.10199, 2021.

Hogle, S. L., Hackl, T., Bundy, R. M., Park, J., Satinsky, B., Hiltunen, T., Biller, S., Berube, P. M., and Chisholm, S. W.: Siderophores as an iron source for picocyanobacteria in deep chlorophyll maximum layers of the oligotrophic ocean, The ISME Journal, 16, 1636–1646, https://doi.org/10.1038/s41396-022-01215-w, 2022.

Holm-Hansen, O.: ATP levels in algal cells as influenced by environmental conditions, Plant Cell Physiol, 11, 689–700, https://doi.org/10.1093/oxfordjournals.pcp.a074557, 1970.

Holm-Hansen, O.: The Use of ATP Determinations in Ecological Studies, Bulletins from the Ecological Research Committee, 215–222, 1973.

Holm-Hansen, O. and Booth, C. R.: The Measurement of Adenosine Triphosphate in the Ocean and Its Ecological Significance, Limnology and Oceanography, 11, 510–519, https://doi.org/10.4319/lo.1966.11.4.0510, 1966.

Honeyman, B. D. and Santschi, P. H.: A Brownian-pumping model for oceanic trace metal scavenging: Evidence from Th isotopes, Journal of Marine Research, 47, 1989.

Honeyman, B. D. and Santschi, P. H.: Coupling adsorption and particle aggregation: laboratory studies of “colloidal pumping” using iron-59-labeled hematite, Environ. Sci. Technol., 25, 1739–1747, https://doi.org/10.1021/es00022a010, 1991.

HOT-DOGS: the Hawaii Ocean Time-series Data Organization & Graphical System [data set], 2025.

Hudson, R. J. M. and Morel, F. M. M.: Distinguishing between extra- and intracellular iron in marine phytoplankton., Limnology and Oceanography, 34, 1113–1120, https://doi.org/10.4319/lo.1989.34.6.1113, 1989.

Hurst, M. P., Aguilar-Islas, A. M., and Bruland, K. W.: Iron in the southeastern Bering Sea: Elevated leachable particulate Fe in shelf bottom waters as an important source for surface waters, Continental Shelf Research, 30, 467–480, https://doi.org/10.1016/j.csr.2010.01.001, 2010.

Karl, D. M.: Cellular nucleotide measurements and applications in microbial ecology, Microbiological Reviews, 44, 739–796, https://doi.org/10.1128/mr.44.4.739-796.1980, 1980.

Karl, D. M.: Total microbial biomass estimation derived from the measurement of particulate adenosine-5’-triphosphate, in: P. F. Kemp, B. F. Sherr, E. B. Sherr, and J. J. Cole [eds.], Handbook of Methods in Aquatic Microbial Ecology, Lewis Publishers, Boca Raton, FL, 359–368, 1993.

Karl, D. M., Björkman, K. M., Dore, J. E., Fujieki, L., Hebel, D. V., Houlihan, T., Letelier, R. M., and Tupas, L. M.: Ecological nitrogen-to-phosphorus stoichiometry at station ALOHA, Deep Sea Research Part II: Topical Studies in Oceanography, 48, 1529–1566, https://doi.org/10.1016/S0967-0645(00)00152-1, 2001.

Karl, D. M., Letelier, R. M., Bidigare, R. R., Björkman, K. M., Church, M. J., Dore, J. E., and White, A. E.: Seasonal-to-decadal scale variability in primary production and particulate matter export at Station ALOHA, Progress in Oceanography, 195, 102563, https://doi.org/10.1016/j.pocean.2021.102563, 2021.

Karl, D. M., Björkman, K. M., Church, M. J., Fujieki, L. A., Grabowski, E. M., and Letelier, R. M.: Temporal dynamics of total microbial biomass and particulate detritus at Station ALOHA, Progress in Oceanography, 205, 102803, https://doi.org/10.1016/j.pocean.2022.102803, 2022.

King, A. L., Sañudo-Wilhelmy, S. A., Boyd, P. W., Twining, B. S., Wilhelm, S. W., Breene, C., Ellwood, M. J., and Hutchins, D. A.: A comparison of biogenic iron quotas during a diatom spring bloom using multiple approaches, Biogeosciences, 9, 667–687, https://doi.org/10.5194/bg-9-667-2012, 2012.

Kok, J. F., Adebiyi, A. A., Albani, S., Balkanski, Y., Checa-Garcia, R., Chin, M., Colarco, P. R., Hamilton, D. S., Huang, Y., Ito, A., Klose, M., Leung, D. M., Li, L., Mahowald, N. M., Miller, R. L., Obiso, V., Pérez García-Pando, C., Rocha-Lima, A., Wan, J. S., and Whicker, C. A.: Improved representation of the global dust cycle using observational constraints on dust properties and abundance, Atmospheric Chemistry and Physics, 21, 8127–8167, https://doi.org/10.5194/acp-21-8127-2021, 2021.

Kuma, K., Nishioka, J., and Matsunaga, K.: Controls on iron(III) hydroxide solubility in seawater: The influence of pH and natural organic chelators, Limnology and Oceanography, 41, 396–407, https://doi.org/10.4319/lo.1996.41.3.0396, 1996.

Kunde, K., Wyatt, N. J., González-Santana, D., Tagliabue, A., Mahaffey, C., and Lohan, M. C.: Iron Distribution in the Subtropical North Atlantic: The Pivotal Role of Colloidal Iron, Global Biogeochemical Cycles, 33, 1532–1547, https://doi.org/10.1029/2019GB006326, 2019.

Landing, W. M. and Bruland, K. W.: The contrasting biogeochemistry of iron and manganese in the Pacific Ocean, Geochimica et Cosmochimica Acta, 51, 29–43, https://doi.org/10.1016/0016-7037(87)90004-4, 1987.

Liu, X. and Millero, F. J.: The solubility of iron in seawater, Marine Chemistry, 77, 43–54, https://doi.org/10.1016/S0304-4203(01)00074-3, 2002.

Lomas, M. W., Baer, S. E., Mouginot, C., Terpis, K. X., Lomas, D. A., Altabet, M. A., and Martiny, A. C.: Varying influence of phytoplankton biodiversity and stoichiometric plasticity on bulk particulate stoichiometry across ocean basins, Commun Earth Environ, 2, 1–10, https://doi.org/10.1038/s43247-021-00212-9, 2021.

Lory, C., Van Wambeke, F., Fourquez, M., Barani, A., Guieu, C., Tilliette, C., Marie, D., Nunige, S., Berman-Frank, I., and Bonnet, S.: Assessing the contribution of diazotrophs to microbial Fe uptake using a group specific approach in the Western Tropical South Pacific Ocean, ISME Communications, 2, 41, https://doi.org/10.1038/s43705-022-00122-7, 2022.

Malmstrom, R. R., Coe, A., Kettler, G. C., Martiny, A. C., Frias-Lopez, J., Zinser, E. R., and Chisholm, S. W.: Temporal dynamics of *Prochlorococcus* ecotypes in the Atlantic and Pacific oceans, The ISME Journal, 4, 1252–1264, https://doi.org/10.1038/ismej.2010.60, 2010.

Marsay, C. M., Barrett, P. M., McGillicuddy Jr., D. J., and Sedwick, P. N.: Distributions, sources, and transformations of dissolved and particulate iron on the Ross Sea continental shelf during summer, Journal of Geophysical Research: Oceans, 122, 6371–6393, https://doi.org/10.1002/2017JC013068, 2017.

Formatted: Font: Not Bold
Formatted: Font: Not Bold
Formatted: Font: Not Bold
Formatted: Font: Not Bold
Formatted: Font: Not Bold
Formatted: Font: Not Bold
Formatted: Font: Not Bold

Moore, C. M., Mills, M. M., Arrigo, K. R., Berman-Frank, I., Bopp, L., Boyd, P. W., Galbraith, E. D., Geider, R. J., Guieu, C., Jaccard, S. L., Jickells, T. D., La Roche, J., Lenton, T. M., Mahowald, N. M., Marañón, E., Marinov, I., Moore, J. K., Nakatsuka, T., Oschlies, A., Saito, M. A., Thingstad, T. F., Tsuda, A., and Ulloa, O.: Processes and patterns of oceanic nutrient limitation, Nature Geoscience, 6, 701–710, https://doi.org/10.1038/ngeo1765, 2013.

Moore, J. K., Doney, S. C., Glover, D. M., and Fung, I. Y.: Iron cycling and nutrient-limitation patterns in surface waters of the World Ocean, Deep Sea Research Part II: Topical Studies in Oceanography, 49, 463–507, https://doi.org/10.1016/S0967-0645(01)00109-6, 2001.

Ohnemus, D. C., Torrie, R., and Twining, B. S.: Exposing the Distributions and Elemental Associations of Scavenged Particulate Phases in the Ocean Using Basin-Scale Multi-Element Data Sets, Global Biogeochemical Cycles, 33, 725–748, https://doi.org/10.1029/2018GB006145, 2019.

Parrington, J. R., Zoller, W. H., and Aras, N. K.: Asian dust: seasonal transport to the hawaiian islands, Science, 220, 195–197, https://doi.org/10.1126/science.220.4593.195, 1983.

Pasulka, A. L., Landry, M. R., Taniguchi, D. A. A., Taylor, A. G., and Church, M. J.: Temporal dynamics of phytoplankton and heterotrophic protists at station ALOHA, Deep Sea Research Part II: Topical Studies in Oceanography, 93, 44–57, https://doi.org/10.1016/j.dsr2.2013.01.007, 2013.

Planquette, H. and Sherrell, R. M.: Sampling for particulate trace element determination using water sampling bottles: methodology and comparison to in situ pumps: Particulate trace element sampling, Limnol. Oceanogr. Methods, 10, 367–388, https://doi.org/10.4319/lom.2012.10.367, 2012.

Price, N. M., Ahner, B. A., and Morel, F. M. M.: The equatorial Pacific Ocean: Grazer-controlled phytoplankton populations in an iron-limited ecosystem, Limnology and Oceanography, 39, 520–534, https://doi.org/10.4319/lo.1994.39.3.0520, 1994.

Prospero, J. M., Savoie, D. L., and Arimoto, R.: Long-term record of nss-sulfate and nitrate in aerosols on Midway Island, 1981–2000: Evidence of increased (now decreasing?) anthropogenic emissions from Asia, Journal of Geophysical Research: Atmospheres, 108, AAC 10-1-AAC 10-11, https://doi.org/10.1029/2001JD001524, 2003.

Rauschenberg, S. and Twining, B. S.: Evaluation of approaches to estimate biogenic particulate trace metals in the ocean, Marine Chemistry, 171, 67–77, https://doi.org/10.1016/j.marchem.2015.01.004, 2015.

Raven, J. A.: Predictions of Mn and Fe use efficiencies of phototrophic growth as a function of light availability for growth and of C assimilation pathway, New Phytologist, 116, 1–18, https://doi.org/10.1111/j.1469-8137.1990.tb00505.x, 1990.

Raven, J. A., Evans, M. C. W., and Korb, R. E.: The role of trace metals in photosynthetic electron transport in O2-evolving organisms, Photosynthesis Research, 60, 111–150, https://doi.org/10.1023/A:1006282714942, 1999.

Redfield, A. C.: The biological control of chemical factors in the environment, American Scientist, 46, 205-222, 1958.

Rii, Y., Karl, D. M., and Church, M.: Temporal and vertical variability in picophytoplankton primary productivity in the North Pacific Subtropical Gyre, Mar. Ecol. Prog. Ser., 562, 1–18, https://doi.org/10.3354/meps11954, 2016.

Rue, E. L. and Bruland, K. W.: Complexation of iron(II1) by natural organic ligands in the Central North Pacific as determined by a new competitive ligand equilibration/adsorptive cathodic stripping voltammetric method, Marine Chemistry, 22, 1995.

Sedwick, P. N., Sohst, B. M., Buck, K. N., Caprara, S., Johnson, R. J., Ohnemus, D. C., Sofen, L. E., Tagliabue, A., Twining, B. S., and Williams, T. E.: Atmospheric Input and Seasonal Inventory of Dissolved Iron in the Sargasso Sea: Implications for Iron Dynamics in Surface Waters of the Subtropical Ocean, Geophysical Research Letters, 50, e2022GL102594, https://doi.org/10.1029/2022GL102594, 2023.

Selph, K. E., Swalethorp, R., R Stukel, M., B Kelly, T., N Knapp, A., Fleming, K., Hernandez, T., and Landry, M. R.: Phytoplankton community composition and biomass in the oligotrophic Gulf of Mexico, J Plankton Res, 44, 618–637, https://doi.org/10.1093/plankt/fbab006, 2022.

Shelley, R. U., Landing, W. M., Ussher, S. J., Planquette, H., and Sarthou, G.: Regional trends in the fractional solubility of Fe and other metals from North Atlantic aerosols (GEOTRACES cruises GA01 and GA03) following a two-stage leach, Biogeosciences, 15, 2271–2288, https://doi.org/10.5194/bg-15-2271-2018, 2018.

Sofen, L. E., Antipova, O. A., Buck, K. N., Caprara, S., Chacho, L., Johnson, R. J., Kim, G., Morton, P., Ohnemus, D. C., Rauschenberg, S., Sedwick, P. N., Tagliabue, A., and Twining, B. S.: Authigenic Iron Is a Significant Component of Oceanic Labile Particulate Iron Inventories, Global Biogeochemical Cycles, 37, e2023GB007837, https://doi.org/10.1029/2023GB007837, 2023.

Steemann Nielsen, E.: The Use of Radio-active Carbon (C14) for Measuring Organic Production in the Sea, Journal du Conseil, 18, 117–140, https://doi.org/10.1093/icesjms/18.2.117, 1952.

Sunda, W. G.: Trace Metal Interactions with Marine Phytoplankton, Biological Oceanography, 6, 411–442, https://doi.org/10.1080/01965581.1988.10749543, 1988.

Tagliabue, A., Aumont, O., DeAth, R., Dunne, J. P., Dutkiewicz, S., Galbraith, E., Misumi, K., Moore, J. K., Ridgwell, A., Sherman, E., Stock, C., Vichi, M., Völker, C., and Yool, A.: How well do global ocean biogeochemistry models simulate dissolved iron distributions?, Global Biogeochemical Cycles, 30, 149–174, https://doi.org/10.1002/2015GB005289, 2016.

Tagliabue, A., Bowie, A. R., DeVries, T., Ellwood, M. J., Landing, W. M., Milne, A., Ohnemus, D. C., Twining, B. S., and Boyd, P. W.: The interplay between regeneration and scavenging fluxes drives ocean iron cycling, Nature Communications, 10, 4960, https://doi.org/10.1038/s41467-019-12775-5, 2019.

Tagliabue, A., Buck, K. N., Sofen, L. E., Twining, B. S., Aumont, O., Boyd, P. W., Caprara, S., Homoky, W. B., Johnson, R., König, D., Ohnemus, D. C., Sohst, B., and Sedwick, P.: Authigenic mineral phases as a driver of the upper-ocean iron cycle, Nature, 620, 104–109, https://doi.org/10.1038/s41586-023-06210-5, 2023.

Tang, D. and Morel, F. M. M.: Distinguishing between cellular and Fe-oxide-associated trace elements in phytoplankton, Marine Chemistry, 98, 18–30, https://doi.org/10.1016/j.marchem.2005.06.003, 2006.

Tovar-Sanchez, A., Sañudo-Wilhelmy, S. A., Garcia-Vargas, M., Weaver, R. S., Popels, L. C., and Hutchins, D. A.: A trace metal clean reagent to remove surface-bound iron from marine phytoplankton, Marine Chemistry, 82, 91–99, https://doi.org/10.1016/S0304-4203(03)00054-9, 2003.

Twining, B. S. and Baines, S. B.: The Trace Metal Composition of Marine Phytoplankton, Annu. Rev. Mar. Sci., 5, 191–215, https://doi.org/10.1146/annurev-marine-121211-172322, 2013.

Twining, B. S., Antipova, O., Chappell, P. D., Cohen, N. R., Jacquot, J. E., Mann, E. L., Marchetti, A., Ohnemus, D. C., Rauschenberg, S., and Tagliabue, A.: Taxonomic and nutrient controls on phytoplankton iron quotas in the ocean, Limnology and Oceanography Letters, 6, 96–106, https://doi.org/10.1002/lol2.10179, 2021.

White, A. E., Giovannoni, S. J., Zhao, Y., Vergin, K., and Carlson, C. A.: Elemental content and stoichiometry of SAR11 chemoheterotrophic marine bacteria, Limnol Oceanogr Letters, 4, 44–51, https://doi.org/10.1002/lol2.10103, 2019.

Wu, J., Boyle, E., Sunda, W., and Wen, L.-S.: Soluble and Colloidal Iron in the Oligotrophic North Atlantic and North Pacific, Science, 293, 847–849, https://doi.org/10.1126/science.1059251, 2001.

Ye, Y. and Völker, C.: On the Role of Dust-Deposited Lithogenic Particles for Iron Cycling in the Tropical and Subtropical Atlantic, Global Biogeochemical Cycles, 31, 1543–1558, https://doi.org/10.1002/2017GB005663, 2017.

Formatted: Font: Not Bold

Formatted: Font: Not Bold

Page 6: [1] Deleted Eleanor S. Bates 3/23/26 1:28:00 PM

Page 6: [1] Deleted Eleanor S. Bates 3/23/26 1:28:00 PM

Page 6: [1] Deleted Eleanor S. Bates 3/23/26 1:28:00 PM

Page 6: [1] Deleted Eleanor S. Bates 3/23/26 1:28:00 PM

Page 6: [1] Deleted Eleanor S. Bates 3/23/26 1:28:00 PM